

The Enigma of GLEAM-X J162759.5-523504.3

Sushan Konar*

NCRA-TIFR, Pune, 411007, India.

*Corresponding author. E-mail: sushan.konar@gmail.com

Abstract. It is proposed that GLEAM-X J162759.5-523504.3, the newly discovered radio transient with an unusually long spin-period ($P_s = 1091.1690$ s), can be identified to be a Radio Magnetar which has a dipolar surface magnetic field of 2.5×10^{16} G. It is shown that - a) it is possible to anchor such a strong field at the core-crust boundary of a neutron star, and b) the energy of field dissipation can explain the observed luminosity (radio & X-ray) of this source.

Key words. radio pulsar—magnetar—fallback accretion—magnetic field

1. Introduction

Since the first (serendipitous) discovery of a neutron star as a radio pulsar (Hewish et al. 1968), some ~ 3500 of them are now known with emissions detected across almost the entire electromagnetic spectrum (Manchester et al. 2005). Despite the wide variety of observational characteristics, these are understood to have three basic modes of energy generation. Accordingly, they can be classified as - a) the rotation powered pulsars (RPP) where rotational energy is lost due to electro-magnetic braking; b) the accretion powered pulsars (APP) where material accretion from a companion gives rise to energetic radiation and c) the internal energy powered (IEP) objects where the emission comes from certain internal reservoirs of energy like the post-formation residual heat or energy stored in ultra-strong magnetic fields (Kaspi 2010; Konar et al. 2016).

Indeed, these classes are neither mutually exclusive, nor are their evolutionary connections unknown. In fact, the connection between the RPP and APP has been studied through the decades and is quite well understood (see Konar (2017) for a review). On the other hand, detailed theory of magneto-thermal evolution and interconnections between different types of isolated neutron stars is being developed in recent years (Pons, Miralles, & Geppert 2009; Kaspi 2010; Viganò 2013). The target objects for this line of investigation include radio pulsars (RPSR), as well as IEP class objects like the Magnetars, the Central Compact Objects (CCO) and the X-ray dim Isolated Neutron Stars (XINS). Already evidence for direct evolutionary connections between the IEPs with RPSRs have started accumulating (Kaspi & Beloborodov 2017; Jawor

& Tauris 2022; Abhishek et al. 2022; Chowhan, Konar, & Banik 2022).

Barring the APPs, the neutron stars are typically observed to have their spin-periods (P_s) and the surface magnetic fields (B_s) within the following range -

- $P_s \sim 1.3 \times 10^{-3} - 23.5$ s,
- $B_s \sim 10^7 - 10^{15}$ G,

with the IEPs predominantly clustering near the upper bounds of both the parameters. However, slow RPSRs, with periods as large as or larger than typical IEPs, have begun to be detected in recent years with advanced observational capabilities. In fact, two RPSRs with the longest periods (of all known neutron stars) - J1903+0433 ($P_s = 14.05$ s) and J0250+5854 ($P_s = 23.54$ s) - have been discovered within the last five years (Han et al. 2021; Tan et al. 2018). Moreover, Magnetar-like X-ray bursts have now been detected from a number of high-magnetic field RPSRs and some of the Magnetars have also been observed to emit periodic radio pulses like RPSRs (these are called ‘Radio Magnetars’). The latest object to join these in-between objects is the radio emitting J0901-4046 with a spin-period of 75.88s and an inferred surface dipolar field of 1.3×10^{14} G (Caleb et al. 2022). Clearly, the boundary between the RPPs and the IEPs is getting blurred.

Quite naturally, the discovery of GLEAM-X J162759.5-523504.3 - a radio transient with an unusually long period of ≈ 1091 s, in the archival data of the ‘Galactic and Extra-galactic All-sky MWA - Extended’ survey has generated great interest (Hurley-Walker et al. 2022). Not only is the period more than an order of magnitude larger than the longest

known before. In combination with other measured parameters, it also makes the identification of this source (within any known neutron star class) extremely difficult.

Therefore, it is of importance to understand the evolutionary history of this source, assuming ‘typical’ values for various parameters at birth. On the other hand, it is also important to know if this source is the first representative of a hitherto unknown class of neutron stars and if so how it connects to other known populations. In the current investigation, we try to look for answers to some of these questions within the current paradigm of neutron star physics.

To begin with, in §2 we enumerate all the measured parameters of GLEAM-X J162759.5-523504.3 (referred to as GLEAM-X hereafter) and discuss the problems of considering this source as a regular RPSR. In §3 we review some of the hypotheses that have been suggested to explain the source (Loeb & Maoz 2022; Katz 2022; Ekşi & Şaşmaz 2022; Gençali, Ertan, & Alpar 2022; Ronchi et al. 2022; Tong 2022). It appears that fallback accretion induced slow-down of a newly born neutron star holds maximum promise for explaining this source. In §4 we discuss the complexities associated with such a scenario. In §5 we offer a simpler solution, in the form of an ultra-strong magnetic field anchored near the core-crust boundary, to the apparent mystery of GLEAM-X. Finally we conclude in §6.

2. Puzzling Parameters

The important observational parameters of GLEAM-X, as reported by Hurley-Walker et al. (2022), are as follows -

- Basic Parameters :
 - $P_s = 1091.1690 \pm 0.0005$ s,
 - $\dot{P}_s \approx 6 \times 10^{-10}$ s/s (best-fit value),
 - brightness variation on timescales $\lesssim 0.5$ s;
- Radiation Characteristics (Radio) :
 - $L_{\text{rad}} \lesssim 4 \times 10^{31}$ erg.s⁻¹ (maximum pulse flux),
 - $T_B \sim 10^{16}$ K,
 - linear polarisation $\sim 88\%$, without any variation with pulse phase or time,
 - two ‘on’ intervals of emission of ~ 30 days with a 26 day null interval in-between;
- Radiation Characteristics (X-Ray) :
 - $L_X \lesssim 10^{32}$ erg.s⁻¹ obtained by Swift XRT;

where, L_{rad} , L_X and T_B denote the radio luminosity, the X-ray luminosity and the brightness temperature respectively.

A consideration of these parameters have given rise to some amount of puzzlement. The main concerns are about - a) the mechanism of energy generation, and b) the reason behind the extremely long spin-period, as discussed below.

Energy Generation : The regularity of emission, combined with brightness variation at time-scales of ~ 0.5 light-second (translates to a region of size 1.5×10^{10} cm), implies that the emission is originating from a rotating compact object. Assuming the source to be rotation powered, we have -

$$\begin{aligned} \dot{E}_R &= -I \omega_s \dot{\omega}_s = 4\pi^2 I P_s^{-3} \dot{P}_s \\ &\lesssim 2.0 \times 10^{28} \text{ erg.s}^{-1}, \end{aligned} \quad (1)$$

where E_R , I and ω_s are the rotational energy, the moment of inertia and the spin angular frequency of a rotating object. Here, E_R is calculated assuming a canonical mass of $1.4 M_\odot$ and radius of 10^6 cm for the neutron star which gives $I_{\text{NS}} \sim 10^{45}$ gm.cm² ($I = 0.4MR^2$ for a uniform density sphere, which a neutron star effectively is). Clearly, this falls short of the actual radio luminosity of GLEAM-X by several orders of magnitude, indicating that the source can not be powered by rotational spin-down alone. Because of this, it has been suggested that the source could be a Radio Magnetar and powered by the decay of its strong magnetic field (Ronchi et al. 2022).

Slow Rotation : The nominal lifetime estimated for the source, assuming a constant surface magnetic field, is -

$$P_s/2\dot{P}_s \approx 3 \times 10^4 \text{ yr}. \quad (2)$$

This is in accordance with the expectation. Because, the upper limit of the X-ray luminosity measured suggests an age greater than $\sim 10^5$ yr (Potekhin et al. 2020). However, the inherent assumption here is that the star slows down due to electro-magnetic braking alone, appropriate for a RPSR. But such a scenario runs into trouble with the energy requirement, as seen earlier. On the other hand, if it indeed is a Magnetar then the assumption of a constant magnetic field becomes problematic.

3. Suggested Scenarios

A number of scenarios have been proposed to explain the peculiarities of GLEAM-X. Here, we describe them

in brief.

Hot Sub-dwarf (HSD) - Loeb & Maoz (2022) hypothesised that GLEAM-X could be an HSD, a stellar core evolving towards a white dwarf phase but not yet fully degenerate, pulsar. Assuming a typical HSD mass of $0.5M_{\odot}$ and radius of $0.3R_{\odot}$ one obtains $\dot{E}_R \approx 3 \times 10^{36} \text{ erg.s}^{-1}$, which is more than sufficient for the energy requirement of GLEAM-X. Moreover, a) the characteristic age and b) the rotation periods are not uncommon amongst HSDs. However, the argument entirely depends on the HSD having a large scale dipolar magnetic field of $\gtrsim 10^8 \text{ G}$. So far, no HSD has been observed to harbour a magnetic field anywhere near this strength.

White Dwarf (WD) - In a somewhat similar vein, Katz (2022) has suggested that GLEAM-X could be a WD pulsar. With $I_{WD} \sim 10^{50} \text{ gm.cm}^2$ (for typical WD mass and radius) one obtains $\dot{E}_R \approx 3 \times 10^{34} \text{ erg.s}^{-1}$, sufficient to power GLEAM-X. Many white dwarfs with P_s as large as a few hundred seconds are also known. Importantly, the Lorentz factor inferred from the temporal substructure of GLEAM-X pulses implying a large radius of curvature (assuming the emission to be caused by curvature radiation) is more in conformity with a white dwarf hypothesis rather than a neutron star one. However, once again, the inferred magnetic field ($\gtrsim 10^{11} \text{ G}$) turns out to be three orders of magnitude larger than the largest field known to exist in white dwarfs (Ferrario, Wickramasinghe, & Kawka 2020).

Precessing Magnetar - A number of Magnetars are known to experience spin precession, with precession periods $\sim 10^{4-5} \text{ s}$, as a result of the deformation of the star caused by strong internal toroidal magnetic fields (Braithwaite 2009). Ekşi & Şaşmaz (2022) consider the measured period of GLEAM-X to be this precession period instead of the actual spin-period. It is not very clear why the slower precession period would show up in the data in exclusion of the (much faster) spin-period itself.

Fallback Disc - The presence of fallback disks around young neutron stars has been invoked to explain a large variety of phenomena in recent years. When a neutron star is born in a supernova explosion some of the explosion ejecta may fail to escape and fall back onto the neutron star. If this material possesses sufficient angular momentum a stable disk can form. Even though the spin evolution of a neutron star is usually determined by the electro-magnetic braking and gravitational wave radiation, it can be significantly affected through the star's interaction with such a disk (Chatterjee & Hernquist 2000; Alpar, Ankay, & Yazgan 2001; Perna et al. 2014; Li et al. 2021). The existence of fall-

back disks has been observationally established by the discovery of such a disk around 4U 0142+61 (Wang, Chakrabarty, & Kaplan 2006).

Ronchi et al. (2022) and Gençali, Ertan, & Alpar (2022) have explained the ultra-long spin-period of GLEAM-X invoking an efficient propeller-phase slow-down of the star through its interaction with the fallback disc. In an accreting system, the pressure of the infalling material is balanced by the stellar magnetic field at the magnetospheric radius (Alfvén radius in a system with spherical symmetry). The motion of the accreting material (charged plasma) is channeled by the magnetic field towards the magnetic poles of the star at distances smaller than this magnetospheric radius. However, if the spin-frequency of the star happens to be higher than the Keplerian angular velocity of the disk at the magnetospheric radius then co-rotation of the infalling matter results in extraction of angular momentum, leading to a slow-down of the star. (We shall discuss the details of this ‘propeller-phase’ in the next section.)

Assuming an initial spin-period of 10ms, an initial crustal magnetic field of 10^{12-15} G and an initial disk accretion rate of $10^{19-29} \text{ gm.s}^{-1}$, Ronchi et al. (2022) have shown that it is possible to slow a neutron star down to GLEAM-X periods through an extended propeller-phase. However, the disk is assumed to become inactive once the required spin-period is reached. An abrupt drop in the accretion rate has been alluded to as the reason for such inactivation. It is not clear why that is likely to happen.

The fallback model developed by Gençali, Ertan, & Alpar (2022) differs from that of Ronchi et al. (2022) in various details. In particular, Gençali, Ertan, & Alpar (2022) take the details of the thermal state of the disk into account. Doing this, they are able to show that the GLEAM-X period can be reached for a specific range of the disk parameters (related to the temperature, the kinematic viscosity and the irradiation efficiency). But, here too the source is expected to arrive at the current period shortly before the disk is inactivated. Thereafter, the evolution of the source would be entirely due to electro-magnetic torque with a $\dot{P}_s \sim 10^{-18} \text{ s/s}$ for a dipolar magnetic field of $\sim 10^{12} \text{ G}$. However, the currently measured source parameters do not appear to agree with a purely electro-magnetic evolution.

4. Problematic Propeller-Phase

To understand the true effect of the disc-field interaction, on a neutron star, detailed modeling is required

which must take many parameters into consideration. However, it is possible to extract some of the important features using simple physical principles. To this end, we use the following values for various neutron star parameters hereafter – $M_{\text{NS}} = 1.4 M_{\odot}$, $R_{\text{NS}} = 10^6$ cm, and $\dot{M}_{\text{Edd}} = 10^{-8} M_{\odot}/\text{yr} \approx 5 \times 10^{17} \text{ gm.s}^{-1}$, where \dot{M}_{Edd} is the Eddington rate of accretion for a neutron star with the above-mentioned mass and radius. We ignore the detailed physical properties of the disk, as well as the nature of the magnetic field (beyond assuming it to be a simple dipole) in this discussion.

Material accretion onto a neutron star is channelised by its strong magnetic field from the Alfvén radius, given by (Pringle & Rees 1972; Ghosh & Lamb 1979) -

$$\begin{aligned} R_A &= (2G)^{-1/7} M_{\text{NS}}^{-1/7} R_{\text{NS}}^{12/7} B_s^{4/7} \dot{M}^{-2/7} \\ &= 1.01 \times 10^{10} B_{15}^{4/7} \left(\frac{\dot{M}}{\dot{M}_{\text{Edd}}} \right)^{-2/7} \text{ cm}, \end{aligned} \quad (3)$$

where, \dot{M} is the disk accretion rate and B_{15} is the dipolar surface magnetic field of the neutron star in units of 10^{15} G.

Plasma flows in along magnetic field lines, that are co-rotating with the star, from the Alfvén radius. This can happen only if the Alfvén radius is less than the light-cylinder radius, R_{LC} , defined to be the radius at which $R_{\text{LC}} \cdot \omega_s$ equals the velocity of light. Here, $\omega_s (= 2\pi/P_s)$ is the spin-frequency of the neutron star. The field lines can not co-rotate with the star beyond this radius. Therefore we must have -

$$R_A \leq R_{\text{LC}}. \quad (4)$$

Using eq.3 this translates into the following relation -

$$B_{15}^{-2} \left(\frac{\dot{M}}{\dot{M}_{\text{Edd}}} \right) \geq 13.80 P_s^{-7/2}. \quad (5)$$

Furthermore, if the Keplerian frequency at Alfvén radius happens to be smaller than the spin-frequency of the star, then the disk material must be spun up for co-rotation. This is achieved by extracting angular momentum from the star, thereby slowing it down. Defining Keplerian radius, R_K , as the radius at which the Keplerian frequency equals the stellar spin-frequency, we obtain -

$$\begin{aligned} \omega_s^2 &= \frac{2GM_{\text{NS}}}{R_K^3} \\ \text{or, } R_K &= \left(\frac{2GM_{\text{NS}}}{\omega_s^2} \right)^{1/3} = 2.11 \times 10^8 P_s^{2/3} \text{ cm}. \end{aligned} \quad (6)$$

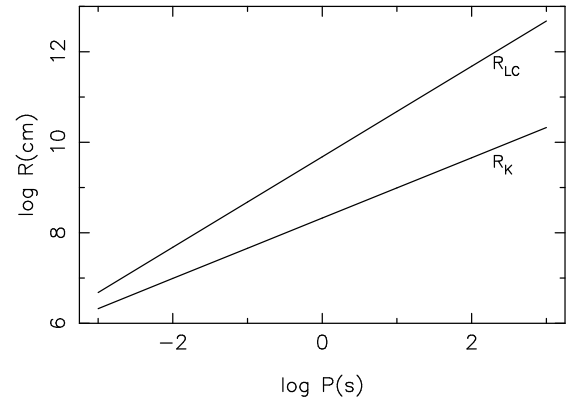


Figure 1: Variation of R_{LC} and R_K with P_s , for a neutron star of mass $1.4M_{\odot}$ and radius 10^6 cm. In the propeller phase, R_A must lie within the limits set by R_{LC} and R_K . See text for details.

At any point in the disk that has a radial distance (from the centre of the star) larger than R_K , the Keplerian frequency would be smaller than the stellar spin-frequency. Therefore, R_A must be larger than R_K for effective angular momentum extraction from the star. In other words, for the propeller phase to be active we must have -

$$R_A \geq R_K. \quad (7)$$

Using eq.3 and eq.6 this gives -

$$B_{15}^{-2} \left(\frac{\dot{M}}{\dot{M}_{\text{Edd}}} \right) \leq 7.59 \times 10^5 P_s^{-7/3}. \quad (8)$$

Combining eq.4 and eq.7 we obtain the following upper and lower limits for R_A required for the propeller phase -

$$R_K \leq R_A \leq R_{\text{LC}}. \quad (9)$$

Fig.[1] shows the variation of R_K and R_{LC} with P_s for a neutron star with our assumed mass and radius. In the propeller phase, R_A must always lie within the limits set by these two lines. It can be seen that the difference between R_K and R_{LC} increases with increasing P_s . At millisecond periods R_{LC} exceeds R_K by a factor of 2-3, but the factor increases to 10 when P_s reaches 10s. Clearly, R_A is limited to smaller intervals at shorter spin-periods compared to those for longer spin-periods.

The full import of this is understood when we combine eq.5 and eq.8 to find the bounds on B_s and \dot{M} for the propeller phase. The condition is obtained as follows -

$$13.80 P_s^{-7/2} \leq B_{15}^{-2} \left(\frac{\dot{M}}{\dot{M}_{\text{Edd}}} \right) \leq 7.59 \times 10^5 P_s^{-7/3}. \quad (10)$$

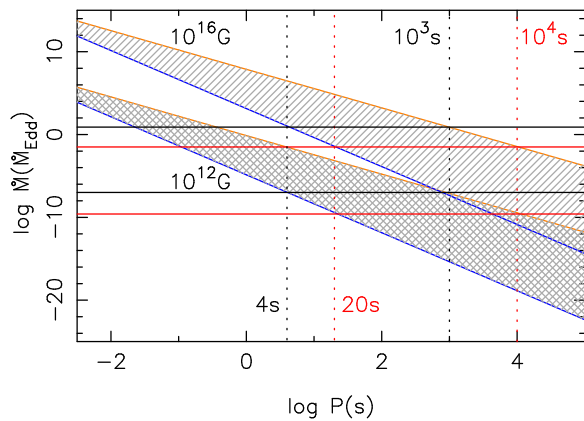


Figure 2: P_s -dependent ranges of \dot{M} in the propeller phase, for constant surface magnetic fields. The shaded areas above and below correspond to magnetic field values of 10^{16}G and 10^{12}G respectively. The vertical broken lines in black correspond to P_s values of 4s and 10^3s , whereas those in orange correspond to P_s values of 20s and 10^4s respectively. The \dot{M} values that can slow a neutron star down from an initial period to a final period are indicated by appropriate horizontal lines - black lines for 4s to 10^3s and orange lines for 20s to 10^4s .

In Fig.[2] we have illustrated this for two values of the dipolar magnetic field. The upper shaded area corresponds to the range of \dot{M} for an assumed field of 10^{16}G and the lower shaded area corresponds to a field value of 10^{12}G . It is immediately seen that, for propeller action, \dot{M} must lie within a specific range which changes rapidly with changing P_s .

It is, of course, possible to achieve a certain amount of slow-down with a constant value of \dot{M} but it depends crucially on the initial spin-period. A very long final period is achievable only for moderately long initial periods. For example, final periods of 10^3s and 10^4s (for objects like GLEAM-X and 1E 161348-5055) are achievable with constant \dot{M} , only from initial periods of 4s and 20s respectively. Also, starting from a given initial period, the maximum slow-down is achieved for a specific value of \dot{M} , which changes significantly with B_s . To bring out the same change in P_s , the \dot{M} required for a 10^{16}G field is about 8 orders of magnitude higher than that required for a 10^{12}G field.

In short, spinning a neutron star down to very long periods, starting with a birth-period in milliseconds (as is normally expected), requires continuous fine-tuning of the accretion rate. Spin-down results in an increase in

$R_K (\propto P_s^{2/3})$. If \dot{M} does not decrease appropriately then at one point R_K would become larger than R_A . When that happens, material would be able to accrete onto the polar regions of the star bringing in additional angular momentum. Instead of propeller induced spin-down this would result in accretion-induced spin-up of the star. On the other hand, if \dot{M} decreases very rapidly then $R_A (\propto \dot{M}^{-2/7})$ may become larger than R_{LC} and the disk would then get disconnected from the star.

In summary, for a constant \dot{M} system, the propeller phase would be short-lived and the final period would be determined by the period at which the system enters the propeller phase. Ultra-long periods would only be attained if the neutron star has already been slowed down significantly (by electro-magnetic braking etc.). On the other hand, if a system goes through an extended period of decreasing \dot{M} , it may oscillate between a propeller and an accretion phase or a propeller and a non-contact phase (unless the rate of decrease of \dot{M} exactly equals the value required for maintaining the system in a continuous propeller phase). However, even if such oscillations finally result in slowing a neutron star down to a period of 10^3s , it may take a much longer time than the estimated age of GLEAM-X.

5. A Mighty Magnetar?

As has been noted in the discovery paper, the extremely large brightness temperature of GLEAM-X implies coherent emission and the high percentage of linear polarisation indicates an ordered magnetic field. Moreover, the nature of the pulse profiles is thought to be suggestive of this source being a Radio Magnetar, even though later work by Erkut (2022) has shown that the spin-down power of GLEAM-X can support its observed radio luminosity like a regular RPP.

It is therefore important to get a measure of the magnetic field of this source. Despite the use of the best-fit value of \dot{P}_s to estimate the spin-down energy, most authors have considered it simply to be an upper limit. However, the exact value of \dot{P}_s itself is of significance.

If one assumes the spin-down to be purely electromagnetic (no observational indication for ongoing accretion) then the surface dipolar field can be estimated to be (Lorimer & Kramer 2004) -

$$B_s = \left(\frac{3c^3}{8\pi^2} \frac{I_{NS}}{R_{NS}^6 \sin^2 \alpha} P_s \dot{P}_s \right)^{1/2} \approx 2.5 \times 10^{16}\text{G}, \quad (11)$$

obtained assuming $\langle \sin^2 \alpha \rangle \sim 1$, where α is the inclin-

ation angle (between the axes of rotation and dipolar magnetic field). This is an order of magnitude larger than the largest magnetic field known for a neutron star (2.06×10^{15} G for J1808-2024, a Magnetar) till now.

Fig.[3] shows all known RPSRs and IEPs for which magnetic field estimates are available. Two death-lines, most relevant for the known neutron star population, have also been shown (see Konar & Deka (2019) for a detailed discussion on the many death-lines extant in the literature and their significance). Both of these death-lines are developed by Chen & Ruderman (1993) and are obtained assuming pair productions ($\gamma + B \rightarrow e^- + e^+$, γ - photon, $e^{-/+}$ - electron/positron, B - magnetic field), required for pulsar emission, to occur predominantly near the polar cap of a neutron star (Ruderman & Sutherland 1975). Assuming - a) the surface field to be dipolar, and b) the radius of curvature of the magnetic field to be approximately equal to the stellar radius, the death-lines are obtained as follows -

$$\mathbf{DL-1} : 4 \log B_s - 6.5 \log P_s = 45.7, \quad (12)$$

$$\mathbf{DL-2} : 4 \log B_s - 6 \log P_s = 43.8; \quad (13)$$

where P_s is in seconds and B_s is in Gauss; with **DL-1** and **DL-2** corresponding to the cases of very curved field lines and extremely twisted field lines respectively.

It can be seen that the majority of the neutron stars are bound by **DL-1** while the rest are bound by **DL-2**, including the slowest pulsar J0250+5854. Only a handful are seen beyond **DL-2** (in particular, the Radio Magnetar J0418+5732 and the millisecond RPSR J1801-3210), and none of these are deep into the pulsar death-valley. It should be noted that these death-lines are not meaningful for APPs and those have therefore been excluded from this figure. It is well known that the X-ray pulsars in HMXBs function far beyond **DL-2** (Konar 2017).

Now, these death-lines correspond to the cessation of pulsar emission due to scarcity of pair-production. Of course, the emission from the IEPs are not necessarily due to such a process (for example, the XINS emission is understood to be caused by the residual heat retained from the supernova explosion). The fact that all non-accreting neutron stars are more or less bound by these death-lines, with most of the IEPs located away from them, simply mean that the RPSRs tend to have the smallest surface magnetic fields for a given value of P_s . Therefore, a Magnetar candidate is ordinarily expected to be located well above **DL-2**. Using the surface field estimated from the best-fit \dot{P}_s , we find that GLEAM-X is located very close to **DL-1**, comfortably above **DL-2**. Moreover, a definite nulling phase has been detected in the radio emission of GLEAM-X and the nulling

pulsars are known to be found predominantly near **DL-1** (Konar & Deka 2019). Considering these, the estimate of B_s (and therefore the best-fit value of \dot{P}_s) does not appear to be completely unreasonable.

We are therefore confronted with two questions - **a)** whether such a strong field can be supported by a neutron star, and, if so **b)** whether it is possible for GLEAM-X to function as a Radio Magnetar.

(a). The maximum stable field anchorable in a neutron star is $\sim 10^{18}$ G (Cardall, Prakash, & Lattimer 2001), if the currents supporting such a field is located deep within the core region. This magnetic field is likely to be in the form of Abrikosov fluxoids, not subject to dissipative processes, in the superconducting core (Shapiro & Teukolsky 1983). Therefore, it is possible for GLEAM-X to function as an RPSR even though its inferred surface field would then be more than two orders of magnitude higher than the highest known for an RPSR (9.36×10^{13} G for J1847-0130).

However, a Radio Magnetar is necessarily powered by the decay of its ultra-strong magnetic field. Therefore, we must consider a crustal field, for which dissipation is possible because of the finite transport coefficients of crustal material (Pons & Geppert 2007; Pons, Miralles, & Geppert 2009; Konar 2017; Pons & Viganò 2019).

The melting temperature ranges from $\sim 10^8 - 10^{10}$ K across the crust. So the crust is likely to be in a crystalline state from almost immediately after the neutron star is formed. This crystal is understood to be composed of unscreened nuclei arranged in a bcc ‘metallic’ lattice with inter-nuclear spacing (varying from $10^{-9} - 10^{-12}$ cm in the density range of $10^8 - 10^{14}$ gm.cm $^{-3}$) exceeding the nuclear size by several orders of magnitude, and therefore to be ‘Coulombic’ in nature.

For the crust to anchor a magnetic field in a stationary configuration, the anisotropic field pressure must be balanced by the non-axisymmetric stresses generated in the crustal solid. Therefore the strongest magnetic field, B_{\max} , that can be supported by the solid crust is -

$$P(B_{\max}) \leq \sigma_{\max}^{\text{shear}}$$

$$\text{or, } B_{\max} \leq \sqrt{8\pi\sigma_{\max}^{\text{shear}}}, \quad (14)$$

where $P(B)$ is the magnetic pressure. The ‘yield’ or shear stress, σ^{shear} , of the crustal solid is given by (Chugunov & Horowitz 2010) -

$$\sigma^{\text{shear}} = \left(0.0195 - \frac{1.27}{\Gamma - 71}\right) \frac{n(Ze)^2}{a}, \quad (15)$$

where, n , a , Z and Γ are the ion number density, the inter-ionic distance (lattice spacing), the atomic num-

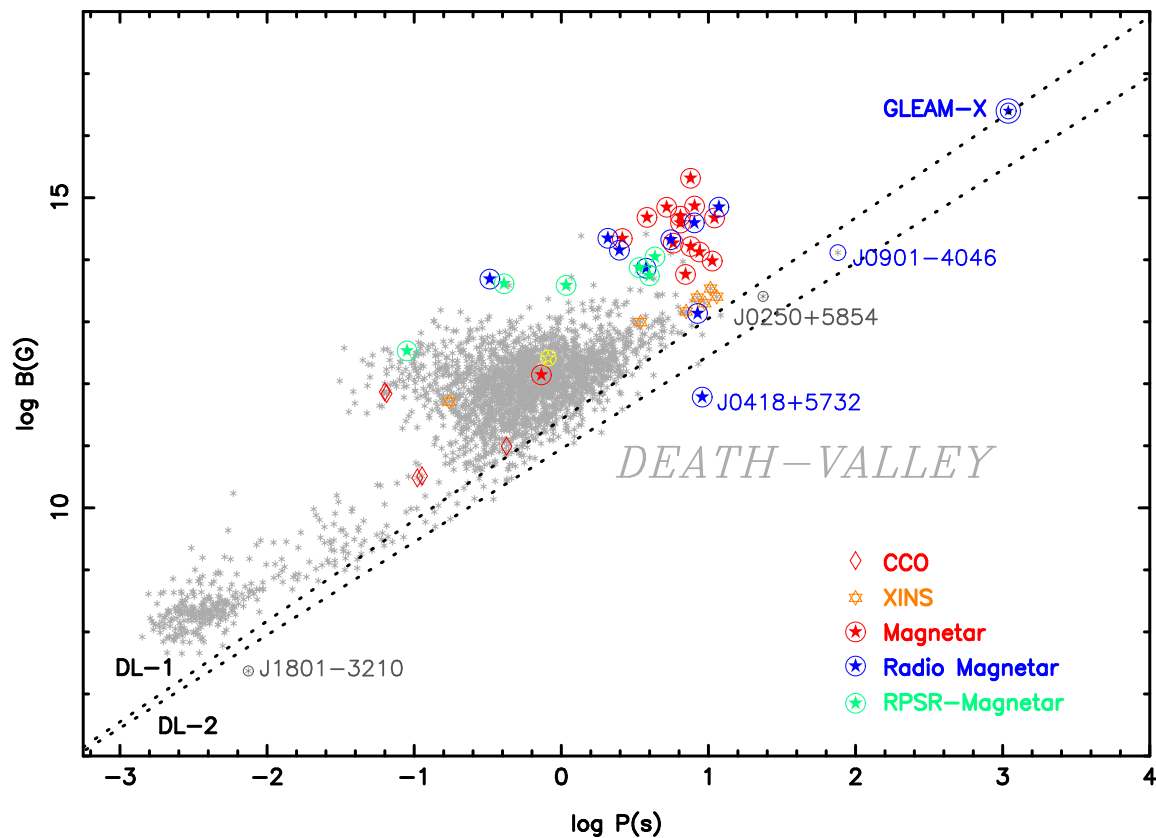


Figure 3: Distributions of RPSRs (grey star) and IEPs, for which B_s estimates exist, in the P_s - B_s plane. Different categories of IEPs (CCOs, XINS, Magnetars) are shown separately, including three types of Magnetars - a) regular Magnetars, b) Radio Magnetars and c) RPSRs with Magnetar like bursts (RPSR-Magnetar). **DL-1** and **DL-2** are two death-lines discussed in the text. J1801-3210 (millisecond RPSR) and J0418+5732 (Radio Magnetar) are two prominent objects on the right of **DL-2**. J0250+5854 is the slowest known RPSR ($P_s = 23.5$ s) and J0901-4046 is the radio neutron star with $P_s = 75.88$ s.

Data Source : a) <https://www.atnf.csiro.au/research/pulsar/psrcat/>,
 b) <http://www.physics.mcgill.ca/~pulsar/magnetar/main.html>,
 c) Gotthelf, Halpern, & Alford 2013; De Luca 2017.

ber of the dominant ionic species (at a given density) and the Coulomb coupling parameter (≥ 250). Clearly, the maximum value of the shear stress, $\sigma_{\max}^{\text{shear}}$, is obtained for the maximum density at the bottom of the crust ($\geq 10^{14}$ gm.cm $^{-3}$), where the dominant ionic species is that of $Z = 20$ (Onsi et al. 2008). Accordingly,

$$\sigma_{\max}^{\text{shear}} \simeq 1.2 \times 10^{32} \text{ dyne.cm}^{-2},$$

or, $B_{\max} \leq 5 \times 10^{16} \text{ G}.$ (16)

Therefore, it is possible for GLEAM-X to have a crustal field of magnitude $2.5 \times 10^{16} \text{ G}$, if it is anchored at the bottom of the crust.

It must be noted that eq.15 has been obtained by the authors for ^{56}Fe matter at a density of 10^9 gm.cm^{-3} . Earlier calculations of σ^{shear} by Strohmayer et al.

(1991), using strain angle estimates of Smoluchowski & Welch (1970), gave much smaller values for σ^{shear} . However, Horowitz & Kadau (2009) and Chugunov & Horowitz (2010) have established that the crust is expected to be much stronger and have much higher values of σ^{shear} . Therefore, it may not be entirely unreasonable to extrapolate the results of Chugunov & Horowitz (2010) to higher densities.

Incidentally, for a self-gravitating object (like a neutron star) any interior magnetic field is also subject to the constraint that the field pressure must always be smaller than the gravitational pressure for the structural stability of the object (Nityananda & Konar 2014; Nityananda & Konar 2015). As things stand today, it is possible for any one of a number of equations of

state to match the observed mass-radius relation of the known neutron stars. However, all of these equations of state have pressures upwards of 10^{33} dyne/cm² for $\rho > 10^{14}$ gm.cm⁻³ (Chamel & Haensel 2008). Consequently, a magnetic field of 2.5×10^{16} G is comfortably accommodated.

In recent years, there have been predictions of a ‘nuclear pasta’ phase in the boundary layer between the crust and the core at densities $\gtrsim 10^{14}$ gm.cm⁻³. Such a layer, though thin, is expected to have much higher resistivity and lower structural strength, compared to a crystalline solid at equivalent densities (Horowitz et al. 2015). Therefore, in presence of such pasta phase, the strongest field would have to be anchored at a somewhat lower density where the crust behaves like a ‘Coulombic’ solid.

(b). Assuming that it is possible to anchor a $\gtrsim 10^{16}$ G field in the crust as discussed above, it is necessary to see if the energy of field decay can power GLEAM-X. The evolution of such a crustal field, in absence of any material motion, is governed by the following equation (Jackson 1975) -

$$\frac{\partial \mathbf{B}}{\partial t} = -\frac{c^2}{4\pi} \nabla \times \left(\frac{\mathbf{1}}{\sigma(\rho, T)} \nabla \times \mathbf{B} \right), \quad (17)$$

where, $\sigma(\rho, T)$ is the electrical conductivity which depends on density (ρ) and temperature (T) of the crustal material. If the currents supporting the field has a small radial extent such that the conductivity can be taken to be constant, the time-scale of field evolution through Ohmic dissipation becomes -

$$\tau_{\text{Ohmic}} = \frac{4\pi L^2 \sigma}{c^2}, \quad (18)$$

where L is the radial extent of the region of current concentration. The density at the bottom of crust is $\gtrsim 10^{14}$ gm.cm⁻³, and the temperature at that depth can be assumed to be $\sim 10^7$ K for a neutron star of age $\lesssim 10^5$ yr. For these parameters, σ is about 10^{28} s⁻¹ for a pure crust, and 10^{25} s⁻¹ for a crust with 5% impurity. If, on the other hand, the bottom layers of the crust remain at a much higher temperature of $\sim 10^8$ K, the conductivity of the pure crust drops to $\sim 10^{25}$ s⁻¹ and the effect of impurity can be ignored at such high temperatures (See Chamel & Haensel (2008) for a detailed discussion on crustal micro-physics.).

Therefore, if we assume the radial extent of the current concentration to be $\sim 10\%$ of the crust, i.e, about 100m, the Ohmic dissipation time-scale turns out to be $\sim 10^6 - 10^9$ yr. Then, the fractional change in the field strength

over the source life-time would be -

$$\frac{\delta B}{B} = \frac{\tau_{\text{GLEAM}}}{\tau_{\text{Ohmic}}} = 10^{-4} - 10^{-1}, \quad (19)$$

where τ_{GLEAM} is the estimated spin-down age of GLEAM-X. In other words, the drop in the field strength would be 10%, at the most. So it can be considered to be effectively constant for all practical purposes.

However, even for such minimal change in the field strength the total energy of dissipation could be quite substantial. The total energy stored in the field can be estimated as follows -

$$E_B = \frac{B^2}{8\pi} 4\pi R^2 L = \frac{1}{2} B^2 R^2 L \sim 10^{52} \text{ erg}, \quad (20)$$

where R is the radius of the star. Therefore, the average rate of field dissipation energy available to the star, over its estimated lifetime, is given by -

$$\frac{\delta E_B}{\tau_{\text{GLEAM}}} \simeq \frac{\delta B B R^2 L}{\tau_{\text{GLEAM}}} \sim 10^{35} - 10^{38} \text{ erg.s}^{-1}. \quad (21)$$

This is far in excess of the maximum observed radio luminosity ($\gtrsim 10^{31}$ erg.s⁻¹) or X-ray luminosity ($\sim 10^{32}$ erg.s⁻¹) of GLEAM-X, as is typically expected for a Radio Magnetar. Therefore, it is entirely possible for GLEAM-X to be a Radio Magnetar, albeit with an ultra-strong magnetic field of $\sim 2.5 \times 10^{16}$ G.

6. Conclusions

The newly discovered radio transient GLEAM-X J162759.5-523504.3 has given rise to a number of conjectures about its nature. Uncertainty regarding the true nature of this source arises primarily because of its ultra-long period and the inadequacy of the inferred spin-down power to explain its current luminosity. Several authors have invoked ‘fallback accretion induced slow-down’ of a newly born neutron star to successfully explain the ultra-long period of this source. However, we find that spinning a neutron star down to very long periods requires continuous fine-tuning of the accretion rate. Otherwise, final periods of 10^3 s are only achievable from initial periods of 4s or larger if the accretion rate remains constant.

In this work, we have considered a simpler solution to the problem, by taking the best-fit value of \dot{P}_s as the true measure of the spin-down rate of the source. Assuming a dipolar spin-down this gives a magnetic field of $2.5 \times$

10^{16} G, an order of magnitude larger than the strongest field known in any neutron star.

However, we are able to demonstrate that -

1. the location of GLEAM-X, in the $P_s - B_s$ plane, is in conformity with other neutron stars of the RPP as well as IEP class,
2. it is possible to anchor such a strong field at the bottom of the crust of a neutron star,
3. the energy of field dissipation is sufficient to explain the observed luminosity (radio & X-ray) of GLEAM-X.

From this, we draw the conclusion that GLEAM-X is most probably a Radio Magnetar with an ultra-strong magnetic field.

It is to be noted that whether a neutron star is powered by spin-down (RPP) or by the decay of its magnetic field (Magnetar), the magnetic field plays a crucial role in its spin-down. In particular, the stronger the field, the faster would be the expected spin-down. Because of this, all the slow neutron stars, discovered recently, possess very strong magnetic fields.

For example, if we consider $10^{14} - 10^{15}$ G fields, the spin-period attained (starting from an initial $P_s \sim$ ms at birth) at an age equivalent to that of the GLEAM-X would be ~ 50 s and ~ 200 s respectively (P_s scales as B). On the other hand, both L_{rad} (obtained from spin-down) and L_X (obtained from field decay) would be down by factors of 10^{-5} and 10^{-3} respectively as they scale as B^2 .

Quite interestingly, this scaling relation works out very well for the newly discovered J0901-4046. Its surface dipolar field and the characteristic age have been estimated to be 1.3×10^{14} G and 5.3 Myr respectively. When these values are used to estimate its current spin-period we obtain ~ 70 s - almost exactly matching the measured period of 75.88s!

7. Acknowledgment

The idea for this work arose out of a couple of lively discussions on GLEAM-X J162759.5-523504.3 during our weekly COD (Compact Object Discussion) where a group of Indian neutron star enthusiasts meet (virtually) to talk about matters of interest.

References

- Abhishek, Malusare N., Tanushree N., Hegde G., Konar S., 2022, arXiv e-prints, arXiv:2201.00295
- Alpar M. A., Ankay A., Yazgan E., 2001, ApJ, 557, L61
- Braithwaite J., 2009, MNRAS, 397, 763
- Caleb M. et al., 2022, Nature Astronomy, 6, 828
- Cardall C. Y., Prakash M., Lattimer J. M., 2001, ApJ, 554, 322
- Chamel N., Haensel P., 2008, Living Reviews in Relativity, 11, 10
- Chatterjee P., Hernquist L., 2000, ApJ, 543, 368
- Chen K., Ruderman M., 1993, ApJ, 402, 264
- Chowhan T. T., Konar S., Banik S., 2022, in Troja E., Baring M., ed, Neutron Star Astrophysics at the Crossroads: Magnetars and the Multimessenger Revolution, Proceedings of IAU Symposium No. 363 (*in press*), arXiv:2201.05248
- Chugunov A. I., Horowitz C. J., 2010, MNRAS, 407, L54
- De Luca A., 2017, in Journal of Physics Conference Series, Vol. 932, Journal of Physics Conference Series, p. 012006
- Ekşi K. Y., Şaşmaz S., 2022, arXiv e-prints, arXiv:2202.05160
- Erkut M. H., 2022, MNRAS, 514, L41
- Ferrario L., Wickramasinghe D., Kawka A., 2020, Advances in Space Research, 66, 1025
- Gençali A. A., Ertan Ü., Alpar M. A., 2022, MNRAS, 513, L68
- Ghosh P., Lamb F. K., 1979, ApJ, 232, 259
- Gotthelf E. V., Halpern J. P., Alford J., 2013, ApJ, 765, 58
- Han J. L. et al., 2021, Research in Astronomy and Astrophysics, 21, 107
- Hewish A., Bell S. J., Pilkington J. D. H., Scott P. F., Collins R. A., 1968, Nature, 217, 709
- Horowitz C. J., Berry D. K., Briggs C. M., Caplan M. E., Cumming A., Schneider A. S., 2015, Phys. Rev. Lett., 114, 031102
- Horowitz C. J., Kadau K., 2009, Physical Review Letters, 102, 191102
- Hurley-Walker N. et al., 2022, Nature, 601, 526
- Jackson J. D., 1975, Classical electrodynamics. Wiley
- Jawor J. A., Tauris T. M., 2022, MNRAS, 509, 634
- Kaspi V. M., 2010, Proceedings of the National Academy of Science, 107, 7147
- Kaspi V. M., Beloborodov A. M., 2017, ARA&A, 55, 261
- Katz J. I., 2022, arXiv e-prints, arXiv:2203.08112
- Konar S., 2017, Journal of Astrophysics and Astronomy, 38, 47
- Konar S. et al., 2016, Journal of Astrophysics and Astronomy, 37, 36
- Konar S., Deka U., 2019, Journal of Astrophysics and Astronomy, 40, 42
- Li S.-Z., Yu Y.-W., Gao H., Zhang B., 2021, ApJ, 907, 87
- Loeb A., Maoz D., 2022, Research Notes of the American Astronomical Society, 6, 27

- Lorimer D. R., Kramer M., 2004, *Handbook of Pulsar Astronomy*
- Manchester R. N., Hobbs G. B., Teoh A., Hobbs M., 2005, *AJ*, 129, 1993
- Nityananda R., Konar S., 2014, *Phys. Rev. D*, 89, 103017
- Nityananda R., Konar S., 2015, *Phys. Rev. D*, 91, 028301
- Onsi M., Dutta A. K., Chatri H., Goriely S., Chamel N., Pearson J. M., 2008, *Phys. Rev. C*, 77, 065805
- Perna R., Duffell P., Cantiello M., MacFadyen A. I., 2014, *ApJ*, 781, 119
- Pons J. A., Geppert U., 2007, *A&A*, 470, 303
- Pons J. A., Miralles J. A., Geppert U., 2009, *A&A*, 496, 207
- Pons J. A., Viganò D., 2019, *Living Reviews in Computational Astrophysics*, 5, 3
- Potekhin A. Y., Zyuzin D. A., Yakovlev D. G., Beznogov M. V., Shibano Y. A., 2020, *MNRAS*, 496, 5052
- Pringle J. E., Rees M. J., 1972, *A&A*, 21, 1
- Ronchi M., Rea N., Graber V., Hurley-Walker N., 2022, *ApJ*, 934, 184
- Ruderman M. A., Sutherland P. G., 1975, *ApJ*, 196, 51
- Shapiro S. L., Teukolsky S. A., 1983, *Black holes, white dwarfs, and neutron stars: The physics of compact objects*. Wiley-Interscience
- Smoluchowski R., Welch D. O., 1970, *Physical Review Letters*, 24, 1191
- Strohmayer T., van Horn H. M., Ogata S., Iyetomi H., Ichimaru S., 1991, *ApJ*, 375, 679
- Tan C. M. et al., 2018, *ApJ*, 866, 54
- Tong H., 2022, arXiv e-prints, arXiv:2204.01957
- Viganò D., 2013, Ph.D. thesis, University of Alicante
- Wang Z., Chakrabarty D., Kaplan D. L., 2006, *Nature*, 440, 772